Seasonal monitoring of cellular energy metabolism in a sentinel species, Dreissena polymorpha (bivalve): Effect of global change?

Fanny Louis, Béatrice Rocher, Iris Barjhoux, Florence Bultelle, Odile Dedourge-Geffard, Véronique Gaillet, Isabelle Bonnard, Laurence Delahaut, Sandrine Pain-Devin, Alain Geffard, et al.

Title: Seasonal monitoring of cellular energy metabolism in a sentinel species, *Dreissena polymorpha* (Bivalve): effect of global change?

Authors: Fanny Louis[1], Béatrice Rocher[2], Iris Barjhoux[1], Florence Bultelle[2], Odile Dedourge-Geffard[1], Véronique Gaillet[1], Isabelle Bonnard[1], Laurence Delahaut[1], Sandrine Pain-Devin[3], Alain Geffard[1], Séverine Paris-Palacios[1], Elise David[1*]

[1] Université de Reims Champagne-Ardenne, INERIS, SEBIO UMR I-02, Reims, France

[2] Université du Havre, INERIS, SEBIO UMR I-02, Le Havre, France

[3] Université de Lorraine, CNRS, LIEC, Metz, France

Keywords: energy, ATP, *Dreissena polymorpha*, biomarkers

Highlights:

- Energy metabolism disturbances were observed from April to June 2019
- Asynchronous spawning between male and female organisms was noticed in 2019
- Markers are potentially proposed in a biomonitoring perspective

Abstract: Aquatic organisms such as bivalves are particularly sensitive to seasonal fluctuations associated with climate changes. Energy metabolism management is also closely related to environmental fluctuations. Changes in both biotic and abiotic conditions, such as the reproduction status and temperature respectively, may affect the organism energy status. A bivalve sentinel species, *Dreissena polymorpha* was sampled along its one-year reproduction cycle *in situ* (2018-2019) to study natural modulations on several markers of energy metabolism regarding seasonal variations *in situ*. A panel of different processes involved in energy metabolism was monitored through different functions such as energy balance regulation, mitochondrial density, and aerobic/anaerobic metabolism. The typical schema expected was observed in a major part of measured responses. However, the monitored population of *D. polymorpha* showed signs of metabolism disturbances caused by an external stressor from April 2019. Targeting a major part of energy metabolism functions, a global analysis of responses suggested a putative impact on the mitochondrial respiratory chain due to potential

pollution. This study highlighted also the particular relevance of *in situ* monitoring to investigate the impacts of environmental change on sentinel species.

*Corresponding author: Fanny LOUIS, fanny.louis@univ-reims.fr

SEBIO, UFR SEN, Campus Moulin de la Housse, BP 1039, 51687 Reims cedex 2, France

1. Introduction

Depending on scenarios, a 0.3 to 0.7°C increase is predicted in the mean Earth surface temperature by 2019 to 2035 (IPCC, 2014). The global climate change also includes the appearance of "exceptional" climatic events. These occurrences also bring important floods or droughts and may have an impact on aquatic populations. Since cellular energy production is dependent on multiple factors such as temperature, food availability or oxygen content (Sokolova et al., 2012), these events could significantly affect the metabolism management of organisms. Indeed, all biochemical and physiological processes are closely related to the amount of energy available within organisms (Frieder et al., 2017; Somero, 2010). Energy metabolism management is also closely related to natural environmental fluctuations. Seasonal temperature variations may lead to the establishment of adaptation and acclimation processes such as metabolic restructuring. Indeed, the aerobic metabolism can be favoured in order to improve the energy available for fitness-related functions including growth and reproduction (Hochaka and Somero, 2002; Salin et al., 2015; Sokolova and Pörtner, 2001; Sokolova et al., 2012). Environmental factors directly modulate cellular and mitochondrial energy management and the energy allocation to vital functions such as maintenance, growth, reproduction and reserves storage (Amiard and Amiard-Triquet, 2008; Hong et al., 2020; Verslycke et al., 2004). In invasive species, reproduction represents a large part of energy allocation (Louis et al., 2019). Seasonal modulations of water physicochemical parameters influence the gonadal maturation and spawning regulation. Fluctuations in energy investment priorities between vital functions have already been observed during the spawning in marine bivalves (Cheung, 1993; Louis et al., 2019; Petes et al., 2008). In this way, natural fluctuations monitoring could be a potential lead to understand energy metabolism management and ATP production in the model species, *Dreissena polymorpha*, along one reproduction cycle.

Mitochondria are the key organelles involved in multiple essential cellular processes (Lane, 2005; Sokolov et al., 2019). They provide more than 90% of cellular ATP and serve as a cellular centre connecting energy metabolism, stress response, signalling and cell survival (Lane, 2007; Monlun et al., 2017; Naquet et al., 2016). Studies on different model species have demonstrated that

mitochondria are particularly sensitive to environmental stressors (Kurochkin et al., 2011; Sokolov et al., 2019; Sokolova et al., 2012). In such context, mitochondria are considered as a stress target and/or the coordinating centre of the adaptive cellular response (Eisner et al., 2018; Sokolova and Lannig, 2008). Positive thermal stress is known to reduce ATP production leading thus to an increase of oxidative phosphorylation (OXPHOS) activity and of reactive oxygen species (ROS) production associated with oxidative damage in bivalve species (Cherkasov et al., 2010; Hraoui et al., 2020; Sokolova et al., 2005). The environmental temperature increase has been associated with a higher respiration rate, leading to a strong proton leak and a gradual mitochondria dissociation in *Crassostrea virginica* (Sokolova and Pörtner, 2001; Sokolova et al., 2005). An increase of mitochondrial damage could also engage the pathway of apoptosis in order to eliminate damage and ensure survival (Vakifahmetoglu-Norberg et al., 2017).

For freshwater risk assessment, integrative biomarkers are required in an active biomonitoring perspective. As the energy metabolism is crucial for all physiological reactions, several studies were realised to develop new energy markers in different model species. The energy cost of metabolism management against environmental disturbances have been discussed in several reviews (Calow, 1991; Calow and Forbes, 1998; Sokolova et al., 2012). The scope for growth and/or the cellular energy charge was investigated in *Dreissena polymorpha* along a pollution gradient (Smolders et al., 2004) or after a metal stress (Louis et al., 2019). These studies pointed out a decrease of the energy allocation to growth and reproduction in presence of stress. Furthermore, the measurement of energy reserves is a useful tool to provide information about the global organism's energy available for maintenance, growth and reproduction (Palais et al., 2011; Sprung, 1995). The adenylate energy charge (AEC) is used as a biomarker of the global health status of the organisms (Le Gal et al., 1997, Smolders et al., 2004). After a chemical contamination, Sokolova et al. (2000, 2005) highlighted the decrease of the AEC in the oyster (*Crassostrea virginica*) and in the White Sea periwinkles (*Littorina spp*).

The zebra mussel, *Dreissena polymorpha* is an invasive filter feeder bivalve widespread in European freshwaters. Due to several biological characteristics such as its abundance, wide geographical distribution and high filtration activity, *D. polymorpha* has been used as a model species

for freshwater biomonitoring for several years (de Lafontaine et al., 2000; Faria et al., 2011, 2009; Kerambrun et al., 2016; Pain and Parant, 2007; Palais et al., 2011). At the cellular level, mitochondria activities are usually reflected by the electron transport system (ETS). Potet et al., (2016) have observed an increase of ETS activity under a metal stress and a decrease after a thermal or dietary stress in *D. polymorpha*. At the molecular level, some units of the OXPHOS were followed (ATP synthase and cytochrome c oxidase). It was shown that the relative gene expression level of ATP synthase increased in summer (Kerambrun et al., 2016).

In this study, cellular energy production (ATP) and management were monitored during one reproduction cycle *in situ*. The whole energy metabolism was targeted through different functions such as energy balance regulation, mitochondrial density and aerobic/anaerobic metabolism. Digestive gland was principally targeted for gene expression and enzymatic activities. Indeed, this organ, similarly to vertebrate liver, play a key role in detoxification mechanisms and has already been noticed as a target for bioaccumulation and biomarker analysis in mollusks (Faggio et al., 2018; Rodrigo and Costa, 2017). Furthermore, most of literature focused on digestive glands concerning biomarker analyses analysis (Faria et al. 2014; Potet et al. 2016, 2018; Louis et al., 2019). In parallel, energy reserves, condition index and the gonadal stage were analysed. As the respiratory chain may be a major source of ROS production, lipid peroxidation content was also measured. Our approach allows a better understanding of the physiology of *Dreissena polymorpha*, under changing natural fluctuations. Energy metabolism studies in *Dreissena polymorpha* are still too few and are only taking in account one or 2 parameters concerning energy management (Louis et al., 2019; Weber et al., 2020). A previous study of our laboratory aimed to characterise the reproduction cycle of the same population of dreissenids. Indeed, Palais et al. (2011) studied *D. polymorpha* gonadal development stage as well as reserves storage for one year. Since this sentinel species is commonly used for *in situ* monitoring, it is essential (1) to characterise the response pattern of monitored markers along the years and (2) to develop new and complemental markers of energy metabolism.

2. Material and Methods

2.1 Organisms collection

Specimens were hand-collected in the Meuse channel (Euville, France, E05°37'28'', N48°44'59'') for one reproduction cycle from May 2018 to June 2019 with a monthly or bimonthly frequency. This site was chosen since data about physiology responses were available on this population of *D. polymorpha* as well as the reproduction cycle characterisation along one year (Palais et al., 2011). Organisms with a length between 15 and 25mm were selected in a depth of 1.5m maximum. Organisms were measured and weighted in order to determine the condition index using the following formula: CI= fresh weight / volume (length x height x width). For gene expression and enzymatic activity analysis (n=12 for each sampling time), digestive glands were dissected and snap frozen. For reserve contents measurement (n=12), the whole organism was dissected and snap frozen. Whole body mussels were frozen for energy nucleotide contents analysis (n=10). All of these procedures were done in the field, except for organisms intended to the gonadal development analysis that were quickly transported to the laboratory in field water (n=12). All marker measurements were realized without taking into account organisms' gender. Dissections and freezing were performed at the sampling site in order to avoid mRNA and protein degradation and to limit marker measurements bias.

2.2 Environmental parameters

At each sampling time, physicochemical parameters were recorded. Water samples (10 L) were carried to the laboratory and processed for analysis in black container. Ammonium (NH_4), nitrates (NO_2), nitrites (NO_3) and chlorophyll a (chl a) contents were measured by spectrophotometric analyses. Chemical oxygen demand and suspended matter were measured by electrochemical and gravimetric methods, respectively. The temperature was recorded every 10min from June 2018 to June 2019 using two probes (TidbiT v2 Temp) installed on the site. The average temperature was calculated for each month.

134 **2.3 Gene expression**

135 Total RNA was extracted from digestive gland using TriReagent (Euromedex) following
136 manufacturer's protocol. RNA integrity was estimated by UV revelation after electrophoresis on 1%
137 agarose gel in TBE (Tris Borate EDTA 0.5%) buffer. RNA purity was estimated by the measurement
138 of the ratio of absorbance at 260 and 280nm. Reverse transcription was performed on 400ng of total
139 RNA using Verso cDNA Synthesis Kit (Thermo Scientific) according to manufacturer's instructions.
140 The reaction was conducted at 42°C for 30min using a PCR Mastercycle (Eppendorf).

141 Gene expression levels were carried out by real-time quantitative PCR using Absolute Blue
142 qPCR SYBR Green ROX Mix (Thermo Scientific) according to the manufacturer's protocol. Specific
143 primers are given in Table 1. Energy balance regulation was studied through *ampk* (AMP-activated
144 protein kinase) and *ampd* (AMP deaminase) gene expressions. Concerning the OXPHOS, three genes
145 were selected: beta subunit ATP synthase (*atp*), cytochrome b (*cytb*), cytochrome c oxidase (*cox*) and
146 succinate dehydrogenase (*sdh*). Another unit of the respiratory chain, the alternative oxidase (*aox*) was
147 recorded. Gene expression levels were also measured for citrate synthase (*cs*) and lactate
148 dehydrogenase (*ldh*), an anaerobic metabolism enzyme. The optimal primer quantity was evaluated
149 across a range of concentrations between 150 and 600nM. Dilutions of the cDNA mixture between
150 1:10 and 1:1000 were tested to calculate the PCR efficiency. The PCR steps consisted in 15 min initial
151 denaturation at 95°C followed by 40 cycles of heat denaturation at 95°C for 10sec, annealing at 60°C
152 for 60sec and were carried out in a CFX Manager (BioRad) on $1/10^{e}$ of ADNc. The relative gene
153 expression level was calculated using the Pfaffl method (Pfaffl, 2001) taking into account the PCR
154 efficiency and normalized by the geometric mean of the two housekeeping genes (actine and
155 ribosomal protein S3) according to Navarro et al. (2011).

156 **2.4 Enzymatic activities**

157 The set of enzymatic activities was individually measured in each mussel. The digestive
158 glands were weighted and crushed in 50mM phosphate buffer containing protease inhibitors (pH 7.6,
159 supplemented with 1mM phenylmethylsulfonyl fluoride and 1mM L-serineborate) at 8:1 (v/w) ratio.

160 Samples were then centrifuged (3000*g*, 10min, 4°C). The supernatant was collected for the enzymatic
161 activity measurement. Assays were performed with an automated spectrophotometer (Galery,
162 ThermoScientific) and with a spectrofluorimeter (SAFAS, Xenius). ETS, lactate dehydrogenase
163 (LDH) as well as proteins content and lipid peroxidation were measured according to Garaud et al.
164 (2016) and Potet et al. (2016). Caspase-3 activity was measured according to Garaud et al. (2016) in
165 cytosolic extract.

166 For cytochrome c oxidase (COX) activity, supernatant was diluted to 1:45 in 100mM Tris
167 buffer (pH 8.1). Reduced cytochrome c at 1mM (Merck) supplemented with 16% of ascorbate (Merck)
168 was added to the previous dilution. Cytochrome c oxidation was then monitored for 3min at 550nm.
169 For citrate synthase (CS) activity, supernatant was diluted to 1:55 in 0.1M Tris buffer (pH 8.1)
170 supplemented with 0.15mM DTNB (Merck) and 0.2mM acetyl co enzyme A (Merck). The activity
171 was first monitored 3min at 420nm. A second measure was performed after the addition of 4mM
172 oxaloacetate (Merck). Enzymatic activity was expressed in $U.g^{-1}$ proteins (molar extinction coefficient
173 (ε) reduced cytochrome c = $7040M^{-1}.cm^{-1}$, ε oxaloacetate = $14140M^{-1}.cm^{-1}$).

174 **2.5 Energy reserve contents**

175 Organisms were weighted and crushed in 50mM phosphate buffer (pH 8) at 5:1 (v/w) ratio.
176 Protein, lipid and glycogen contents were measured on the homogenate. Protein content was
177 determined by the Bradford's method. Lipid and glycogen contents were measured according to the
178 method of Van Handel (1985) and adapted by Plaistow et al. (2001). Results were expressed in $mg.g^{-1}$
179 of fresh weight (FW).

180 **2.6 Energy nucleotide contents**

181 Nucleotides extraction was realised as described by Sokolova et al. (2005). Briefly, frozen
182 mussels were quickly dissected and lyophilized for 48h. Samples were then crushed in 0.6M
183 perchloric acid (Merck) solution, centrifuged (3000*g*, 10min, 4°C) and the supernatant was collected.
184 The pH of each extract was adjusted to 5 - 6.5 with 5mM potassium hydroxide and 1M bicine solution.
185 Precipitated potassium perchlorate was removed by a second centrifugation. Extracts were then

186 filtered (0.45µM) and stored at -80°C. Concentrations of ATP, ADP, AMP and IMP were measured
187 with an HPLC system and Nucleosic C18 column (Nucleosil) according Sokolova et al. (2005). The
188 separation was performed at a flow rate of 0.8ml.min^{-1} using a mobile phase of 1M phosphate buffer
189 with 5% methanol (pH 6) for 15min. Nucleotide contents were monitored at 254nm and nucleotide
190 quantifications were calculated using ATP, ADP, AMP and IMP standards (Sigma) of 20, 10, 2 and
191 10µM, respectively.

192 Adenylate energy charge (AEC) was calculated from the tissue concentrations of adenylates as
193 follows:

194 $$AEC=\frac{[ATP]+0.5\times[ADP]}{[ATP]+[ADP]+[AMP]}$$

195 **2.7 Gonadal development analysis**

196 Dissected organisms (without byssus and shell) were fixed in Bouin's aqueous solution for
197 24h followed by successive alcohol dehydration baths from 50° to 100°. After deshydratation, sampled
198 were placed in a butanol solution in order to permeate all tissues. Samples were then paraffin-
199 embedded and 7µM sections were prepared from the foot to gonads of organisms. Sections were
200 stained with picro indigo carmin and solid nuclear red and observed with a microscope to sex the
201 gonadsand to assign them to a development stage (Gist et al., 1997; Palais et al., 2011). This method
202 was based on the size and the number of present oocytes as well as spermatogenesis steps.

203 **2.8 Statistical analysis**

204 Marker responses were analysed by a one-way ANOVA to assess time effect. Parametric
205 (Tukey) or non-parametric (Kruskal-Wallis) post-hoc tests were processed on markers and obtained *p*-
206 values were adjusted for multiple comparisons by a correction method (Benjamini and Hochberg).
207 Normality and homoscedasticity of the data were tested with Shapiro and Bartlett tests respectively.
208 Correlations were performed on the total data set. A clustered map was built on a complete linkage
209 using Euclidean distance measures between different variables. The obtained values can be seen as a
210 robust approximation of the Pearson correlation. A global analysis of biomarker results was also
211 performed with a Partial Least Square Discriminant Analysis (PLS-DA) to identify the overall

capacity of biomarkers to discriminate the months and to define the most relevant markers among the battery. Relevance of marker responses was based on the individual role of each marker in the overall model, estimated by the VIP (Variable Importance in the Projection). Only markers with a VIP > 1 were considered significant in the model (PLS-DA). Since only four organisms could be sampled in February (used for gene expression) and 16 in March 2019 (4 for gene expression, 4 for enzymatic activity, 4 for nucleotide contents and 4 for histology), the results obtained for these months are presented in the different figures but the data were excluded for statistical analysis. A threshold of $p < 0.05$ was considered significant. Statistical analyses were performed using R software (R Development Core Team, 3.5.0).

3. Results

3.1. Environmental parameters

Water physicochemical features are reported in Table 2 and Fig. 1. Water temperature varied seasonally, the lowest values were recorded in fall (November) and the highest values were recorded in summer (August). Strong daily temperature variations were observed in August (5°C min - 30°C max) and November (-2°C min – 20°C max). In 2019, suspended matter values were higher than in 2018 as well as the mean of nitrates contents. May and June 2019 chl a levels were not detected. All physicochemical parameters measured along the study complied with the framework directive on water (2000/60/CE, 2000).

3.2. Reproduction cycle

Gonadal development stages are presented in Fig. 2. Since only one male was observed in November 2018 in histological analysis, the male gonadal index could not be determined. In 2018, males spawned their gametes between July and September (Fig. 2A) and females between May and August (Fig. 2B). The spawning events were synchronous for both sexes in 2018. Females' gonadal development seemed to be more premature than males' development in 2019. A shift was observed between males and females' gonadal stage between April and June 2019. Indeed, the spawning of

oocytes began in April when males were halfway between maturation and pre-spawn stage. In addition, in June 2019, all the females had spawned their gametes whereas no male had spawned theirs. It is also necessary to take into account the sampling randomness resulting in a sex ratio rarely equals to 1:1.

3.3. Global health status

Condition index (CI) (Fig. 3A), lipid and protein contents (Fig. 3C-D) showed globally the same response variations. CI values decreased just after the spawning (July and August 2018) and then gradually increased until the next reproduction period (from September 2018 to April 2019). Lipid contents also decreased in reproduction period (from August to November 2018) and increased from April 2019. Although protein content variations were less marked, it decreased during the gametes spawning and then increased again. Concerning glycogen reserves (Fig. 3B), a significant decrease was observed in August 2018 followed by a significant increase until November 2018 (5-10mg.gFW^{-1}). From April 2019, glycogen content reached the same level as in August 2018 (< 2mg.gFW^{-1}).

3.4. Mitochondria efficiency

Mitochondria efficiency was assessed in our study by the OXPHOS and the citrate synthase activity and transcriptional level. CS activity increased during the pre-reproduction and reproduction periods while trend to decrease during post reproduction and rest (Fig. 4A). Concerning COX activity, a significant decrease since April 2019 was observed (Fig. 4B). The ETS activity showed a 2-fold increase in June 2018 and came back to lower level in July and August (Fig. 4C). A gradually increase was then observed from September 2018 to June 2019. Globally, relative gene expression levels exhibit two distinct patterns. OXPHOS subunits genes (*cox*, *atp* and *cytb*) reach their highest levels during the pre-reproduction and reproduction periods while they exhibited a marked decrease during post reproduction and rest periods (Fig. 5A-B-C). On the contrary, citrate synthase gene expression (*cs*) level was significantly higher during the rest period (Fig. 5D). No difference of *sdh* relative gene expression level could be noticed along the year (Fig. S1).

3.5. Energy balance

Energy balance regulation was studied through *ampk* and *ampd* gene expressions (Fig. 6). The transcript levels of *ampk* (Fig. 6A) gradually increased from May 2018 to November 2018 and decreased significantly in April 2019. Levels stayed low until June 2019. Although no significant difference could be observed, the expression of *ampd* gene (Fig. 6B) showed the same pattern of variation. ATP and ADP contents presented a similar progression over the year than *ampk* and *ampd* gene expression levels (Fig. 7, part I: A-B). Energy nucleotides concentration was stable from May 2018 to September 2018. A strong increase was observed in November 2018 followed by an important reduction of ATP and ADP contents in April 2019. The pattern of AMP and IMP contents were similar but they slightly differed from the previous markers (Fig. 7, part I: C-D). Indeed, the concentration of these nucleotides were stable from May 2018 to August 2018 and gradually increased until April 2019 where they reached a steady state ($p < 0.05$). A correlation was observed between ATP content and the expression of *ampd* involved in energy balance regulation but also with *cs* gene expression, glycogen and lipid contents (Table S1). The AEC remained stable from May 2018 to November 2018 (0.5-0.7). Nevertheless, a significant decrease was observed in April 2019 (0.13-0.32) (Fig. 7, part II).

3.6. Stress markers

Anaerobic metabolism was assessed through *ldh* gene expression and LDH activity, both presenting a similar pattern of responses (Fig. 8 A-B). Values were higher in pre-reproduction and reproduction periods than during post-reproduction and rest periods. A gradual increase of *aox* relative gene expression was observed from May 2018 to August 2018 and it decreased until June 2019 (Fig. 8C). On the contrary, lipid peroxidation (LOOH) content was stable from May 2018 to November 2018, while it displayed a significant increase from April 2019 compared to July and August 2018 (Fig. 8D). LOOH concentration was negatively correlated with condition index, energy reserves (lipids and glycogen). Positive correlations were also observed between LOOH and LDH activity and AMP/IMP contents (Table 3). Caspase-3 (CSP3) activity was measured only on 7 sampling times

(May, June, July, August and November 2018 and May and June 2019). Its activity increased significantly from November 2018 to June 2019 (Fig. 8E). Negative correlation between CSP3 activity and *cytb* gene expression was noticed while positive correlation with stress markers like LOOH measurements ($r^2 = 0.57$, $p < 0.05$) and IMP/AMP contents were observed (Table 3).

3.7. Global analysis

A PLS-DA model was built and explained 68.2% of between-month variance with the two first axis. The first three VIP markers were *atp*, *cs* and *ldh* gene expressions (Table S2). Caspase-3 activity was excluded of the total data set.

The PLS model built explained 70.6% of between physico-chemical parameters variance with the two first axis. PLS allowed us to identify the importance of each parameter on biological responses. A clustered map was then built. The rows and columns were reordered according to hierarchical clustering method to identify interesting patterns. According to the cluster results (Fig. 9), stress markers as LOOH and IMP content, condition index and LDH activity were strongly positively correlated with suspended matter, nitrate and oxygen contents and negatively correlated with temperature and the content of ammonium. Conversely, *aox* gene expression was negatively correlated with suspended matter and oxygen content and positively correlated with temperature and the content of ammonium. Furthermore, cluster results highlighted that environmental parameters such as nitrites and chl a content had no effect on biological responses along the reproductive cycle. Some biological responses as *sdh*, *cox*, *cs*, *ampd*, *atp* relative gene expression and ATP content were not influenced by measured environmental parameters.

4. Discussion

The aim of this study was to understand the effect of natural fluctuations and intrinsic variations on global energy metabolism in the model species *Dreissena polymorpha in situ*.

4.1. Global status

According to our observations, *D. polymorpha* exhibited a typical annual reproductive cycle with a gonad development phase during fall, a maturation and spawning phase in spring–summer and, if present, a resting phase at the end of the summer (males). These observations are consistent with the reproductive patterns previously described in *D. polymorpha* populations (Binelli et al., 2004; Juhel et al., 2006; Mackie and Ontario, 1990; Palais et al., 2011). In 2019, the expected reproductive cycle was observed but the reproduction period was asynchronous between males and females. No reason was bringing out to explain this observation. Indeed, natural media are continuously submitted to several perturbations. This asynchronous spawning could be a consequence of a potential pollution or an accumulation of different exceptional events like drought or flood periods. Concerning energy reserves, lipid content followed the reproduction cycle with a significant decrease in August 2018 concurrently with gamete emission, similarly to what is reported by Kwan et al. (2003), Hassan et al. (2018) and Hong et al. (2020). Since females were mostly represented in our samples for histology analysis, the high lipid content observed until April 2019 might be explained by the accumulation of lipid nutrients in the oocytes (Palais et al., 2011). According to our results, glycogen content increased after spawning of the gametes and decreased in April 2019. Tourari et al. (1988) shown that glycogen was largely used for the formation of the gametes and the gonadal tissues during gametogenesis and is especially converted into lipid materials in maturing oocytes in *Dreissena polymorpha*. These observations were also highlighted in oysters through an increase of glycogen content in pre-reproduction period followed by a net decrease during the spawning one (Hong et al., 2020). However, in our study, glycogen storage was significantly lower from April to June in 2019 compared to the same period in 2018. Reproduction cycle and glycogen content observations did not follow the schema described for *Dreissena polymorpha* and others bivalves' species (Hong et al., 2020; Palais et al., 2011; Ram et al., 1996, 1993). Glycogen might have been used simultaneously for the gamete development and spawning as well as for other cellular energy demands since glycogen is a main source of energy in organisms (Anacleto et al., 2013; Andrade et al., 2017; Cordeiro et al., 2016, 2017).

338 **4.2. Energy metabolism**

339 Globally, energy metabolism appeared to be more active during the pre-reproduction and the
340 reproduction periods than during the post-reproduction and rest periods. The respiratory chain units
341 (i.e. *cox*, *atp*, and *cytb* gene expressions) presented the same pattern of responses as the anaerobic
342 metabolism markers (*ldh* gene expression and LDH activity). Study of the ETS activity during two
343 years on *D. polymorpha* showed similar responses with an increase of the activity from May to June of
344 each year (Fanslow et al., 2001). According to our results of *ampk* relative expression level, a
345 significant decrease was observed from April 2019 compared to November 2018. An accumulation of
346 AMP was simultaneously measured in the organisms. As the AMPk is activated by high AMP
347 concentrations (Chauhan et al., 2020; Fredrich and Balschi, 2002), the decrease of *ampk* relative
348 expression might be the result of a negative feedback. This negative feedback could also be applied to
349 the *ampd* relative gene expression modulation as this enzyme is activated by AMP intracellular
350 concentration too (O'Brien et al., 2017; Składanowski et al., 2005). Higher production of ATP should
351 be observed consequently to counterbalance AMP accumulation and maintain a positive energy
352 balance. However, in our study, a significant decrease in ATP content was observed from April 2019
353 while ETS activity seemed to remain stable. The oxygen consumed in the mitochondria is directly
354 linked to the flow of electrons and the synthesis of ATP by the ATPsynthase. However, part of this
355 flow can be shunted by an alternative route which bypasses the respiratory chain before complex III.
356 Hence, especially in the presence of low levels of COX activity, the electron transport system
357 contributes less to the driving force of the protons, and from there to the production of ATP. Thus
358 from March to April 2019, the AOX activity could maintain the ETS level in parallel with a decrease
359 in the ATP level. All these observations suggesting thus an imbalance of the energy metabolism.

360 The observed increase in IMP and AMP concentrations may activate glycogen phosphorylase
361 and further enhance glycolysis and the tricarboxylic acid (TCA) cycle when the demand for ATP
362 production increases (Han et al., 2016). Decreased glycogen content observed could be a consequence
363 of the accumulation of IMP and AMP in organisms. CS catalyses condensation of the acetyl group of
364 acetyl-CoA with oxaloacetate forming citrate. It represents the first step of the TCA cycle (Eprintsev

et al., 2018). Products provided by TCA cycle are then used by the respiratory chain in order to produce ATP. In our study, CS activity increased during the pre-reproduction and reproduction periods as well as *atp*, *cytb* and *cox* relative gene expression levels. These results were already observed through an *atp* and *cox* relative expression increasing during spring and/or summer (Kerambrun et al., 2018; Navarro et al., 2011). These results suggest an increase in the respiratory chain functioning during pre-reproduction and reproduction periods. Although it is difficult to compare a gene expression with the activity of the corresponding enzyme, a global suppression of the metabolic rate was observed when all biological responses are considered. Indeed, COX activity and ATP content decreased significantly while ETS activity and LOOH measurements increased from April 2019 to June 2019. Meanwhile, the caspase-3 (CSP3), a protease involved in apoptosis, was significantly more active. In addition, CSP3 activity was also correlated with the expression of OXPHOS-related genes and IMP concentrations. Caspase activation and apoptosis are associated with a decline in ATP levels and a production of reactive oxygen species (ROS) (Ricci et al., 2004; Sharma et al., 2017). The changes in metabolic processes and CSP3 activity suggest an activation of apoptosis pathway likely resulting from a global stress.

4.3. A global response overview

The multivariate analysis allowed us to consider the modulations of the whole panel of markers. This method showed that some markers were positively or negatively correlated with environmental parameters. The contents of IMP and LOOH, and LDH activity are modulated by stressing conditions (Falfushynska et al., 2014; Lushchak, 2011). LDH activity is a marker of global stress whereas lipid peroxidation is used as an indicator of oxidative stress. AMP deaminase protein catalyses the hydrolysis of AMP to form IMP and ammonia. AMPd and AMPk proteins play a role in the energy balance and its regulation. An intracellular AMP content increase reflects an enhanced use of ATP. To avoid the accumulation of AMP, the AMPd converts it into IMP thus suggesting that some stress is challenging the organisms (Lushchak, 2011). In our study, these markers were correlated to all analysed environmental factors except for chl a and nitrite contents. Moreover, lipid peroxidation was positively correlated with IMP and lipid concentrations. The global health status of the organisms

seemed to be affected *in situ* through the induction of stress markers like IMP and LOOH. According to our global analysis, suspended matter and nitrate concentrations seemed to be associated with an impact on energy metabolism of *D. polymorpha*.

4.4. Exceptional events: a long-term impact?

There was a significant increase in the frequency and the intensity of meteorological and hydrological events (EEA, 2007). In the Meuse department, drought periods were recorded in summer 2018 and 2019. The year 2018 was characterized by an exceptional drought that led to placing the entire department in a situation of alert that was extended from August to December. This prefectural decree was renewed in summer 2019 (Decree of the 8th August 2019 on the water use). Drought events may have more effects than flood periods on aquatic organisms due to their duration and large spatial impacts (Hrdinka et al., 2012). The decrease in the water column height leads to a more drastic increase in water temperature (van Vliet and Zwolsman, 2008). According to our *in situ* observations in summer 2018, the temperature stayed above 25°C during three weeks in July and August. *D. polymorpha* is an ectotherm organism with a lethal temperature in acute stress between 35°C and 37°C (Spidle et al., 1995). Several studies reported optimal temperatures for the reproduction, the development and the survival of *D. polymorpha* between 10°C and 20°C (bij de Vaate et al., 2002; Ram et al., 1993; Sprung, 1995). Drought periods observed may also have an impact on the physiology of organisms. Seasonal acclimation to different temperatures changes the tolerance window for invertebrates due to a switch in energy metabolism management in order to assure vital functions related to the fitness (Jost et al., 2015; Lannig et al., 2006; Sokolova et al., 2000). Based on our results, in 2018, temperature varied up to 20°C (November) and 25°C (August) in one day. Populations of *D. polymorpha* are usually hand-sampling close to the shore. These populations are also submitted to the strong variations that may have an impact on physiology of mussels, changing thus their global status. Temperature is also known to have a synergic effect together with contaminants (Cherkasov et al., 2010; Lannig et al., 2006; Soon and Zheng, 2019). Energy cost caused by natural fluctuations and exceptional events repetition might make organisms more vulnerable to anthropic pollution at long term and impact population dynamics.

4.5. Water physicochemistry and biological responses: a potential pollution?

Physicochemical parameters like pH, temperature and ion concentrations (NO_3^-, PO_4^{3-}) are known to regulate the distribution of *D. polymorpha* populations (McMahon, 2002; Ramcharan et al., 1992). The values recorded for pH and temperature in the Meuse channel from May 2018 to June 2019 were consistent with the ecological requirements of the species (Ramcharan et al., 1992). However, a peak of nitrate and phosphate concentrations (31mg.L^{-1} and 0.126mg.L^{-1} respectively) was noticed in December 2018 in the Meuse channel 20km from the sampling site. These concentrations remained stable until February 2019 (31-25.96mg.L^{-1} NO_3^- and 0.120-0.114mg.L^{-1} PO_4^{3-}) (French Water Agency data and Table 2). According to the Water Framework Directive, a maximum concentration of 50mg.L^{-1} of nitrates is defined as a threshold for a "good" ecological status by the regulation (2000/60/CE, 2000). However, studies showed that effects on aquatic fishes might be observed at lower concentrations after 30 days of exposure (Camargo et al., 2005). Alonso and Camargo (2003) exposed the mollusc *Potamopyrgus antipodarum* to N-NO_3^- to evaluate the LC_{10} at 24, 48, 72 and 96h. The calculated LC_{10} values were divided by 2 between 24h (1128 ppm) and 96h (585 ppm) of exposure. Similar observations were highlighted after a 14-days chronic exposure with a LC_{50} divided by 10 between 1 and 14 days (Benítez-Mora et al., 2014). Camargo et al. (2005) concluded that LC measured values may be divided by a factor 18 to 20 between acute and chronic exposures. However, to our knowledge, no data are available on the effect of nitrates in *D. polymorpha*. Simultaneous presence of nitrates and orthophosphates is known to reflect a pesticides pollution (Majumdar and Gupta, 2000). Based on the DCE legislation, the limit of pesticides emission is 0.5mg.L^{-1} in freshwaters (2000/60/CE, 2000). In December 2018, total pesticides concentration was 0.495mg.L^{-1} (French Water Agency data). Several pesticides targeting the mitochondria, and especially the respiratory chain, are extensively found in freshwaters. Nevertheless, more information would be necessary to approve the hypothesis of a potential pesticide impact on organism's mitochondria.

5. Conclusion

This study bring deeper knowledge in the management of energy metabolism in a sentinel species, *D. polymorpha*, in order to develop new potential biomarkers in a biomonitoring perspective. According to our results, three genes involved in ATP production could constitute potential biomarkers. Indeed, *sdh*, *atp* and *cs* genes expression were not influenced by natural seasonal fluctuations. Complementary studies are necessary to confirm their relevance as potential biomarkers. Targeting a major part of energy metabolism and globally analysing their responses allowed us to suggest a putative impairment of mitochondrial respiratory chain, likely resulting from an *in situ* perturbation. Indeed, the monitored population of *D. polymorpha* seemed to be impacted by an external stress from April 2019. Natural environments are subjected to multiple stressors and it is impossible to know the origin of the perturbations. However, flood and drought periods associated with high temperature variations in only one day or during several days may sensitize the organisms to potential chemical stress and could affect vital functions. The asynchronous gonadal development between males and females observed in 2019 as well as the metabolic depletion could be a consequence of exceptional climatic events associated with the pollution. Beyond the characterisation of the energy metabolism management in *D. polymorpha* along one reproduction cycle, this study highlighted the relevance of *in situ* monitoring in particular to investigate the impact of global change on sentinel species.

Acknowledgment

We wish to thank Danièle Pauly for her valuable help for caspase-3 activity measurements as well as the LIEC in Metz for its welcome. This work was supported by the Grand-Est region and the University of Reims Champagne Ardenne through MEENDRE project.

References

Amiard, J.C., Amiard-Triquet, C., 1998. Les biomarqueurs de dommages. In: Les biomarqueurs dans l'évaluation de l'état écologique des milieux aquatiques, Chap 3. Lavoisier.

Alonso, A., Camargo, J.A., 2003. Short-Term Toxicity of Ammonia, Nitrite, and Nitrate to the Aquatic Snail *Potamopyrgus antipodarum* (Hydrobiidae, Mollusca). Bulletin of Environmental Contamination and Toxicology 70, 1006–1012. https://doi.org/10.1007/s00128-003-0082-5

Arrêté du 8 août, 2019. Arrêté du 8/08/19 relatif aux mesures de restrictions aux usages de l'eau en vue de la préservation de la ressource en eau dans le département de la Meuse, arrêté préfectoral n° 2019-7228.

Benítez-Mora, A., Aguirre-Sierra, A., Alonso, Á., Camargo, J.A., 2014. Ecotoxicological assessment of the impact of nitrate ($NO3^-$) on the European endangered white-clawed crayfish *Austropotamobius italicus* (Faxon). Ecotoxicology and Environmental Safety 101, 220–225. https://doi.org/10.1016/j.ecoenv.2013.12.025

bij de Vaate, A., Jazdzewski, K., Ketelaars, H.A.M., Gollasch, S., Van der Velde, G., 2002. Geographical patterns in range extension of Ponto-Caspian macroinvertebrate species in Europe. Canadian Journal of Fisheries and Aquatic Sciences 59, 1159–1174. https://doi.org/10.1139/f02-098

Binelli, A., Bacchetta, R., Mantecca, P., Ricciardi, F., Provini, A., Vailati, G., 2004. DDT in zebra mussels from Lake Maggiore (N. Italy): level of contamination and endocrine disruptions. Aquatic Toxicology 69, 175–188. https://doi.org/10.1016/j.aquatox.2004.05.005

Calow, P., 1991. Physiological costs of combating chemical toxicants: Ecological implications. Comparative Biochemistry and Physiology Part C: Comparative Pharmacology 100, 3–6. https://doi.org/10.1016/0742-8413(91)90110-F

Calow, P., Forbes, V.E., 1998. How do physiological responses to stress translate into ecological and evolutionary processes? Comparative Biochemistry and Physiology Part A: Molecular & Integrative Physiology 120, 11–16. https://doi.org/10.1016/S1095-6433(98)10003-X

Camargo, J.A., Alonso, A., Salamanca, A., 2005. Nitrate toxicity to aquatic animals: a review with new data for freshwater invertebrates. Chemosphere 58, 1255–1267. https://doi.org/10.1016/j.chemosphere.2004.10.044

Chauhan, A.S., Zhuang, L., Gan, B., 2020. Spatial control of AMPK signaling at subcellular compartments. Critical Reviews in Biochemistry and Molecular Biology 1–16. https://doi.org/10.1080/10409238.2020.1727840

Cherkasov, A.S., Taylor, C., Sokolova, I.M., 2010. Seasonal variation in mitochondrial responses to cadmium and temperature in eastern oysters *Crassostrea virginica* (Gmelin) from different latitudes. Aquatic Toxicology 97, 68–78. https://doi.org/10.1016/j.aquatox.2009.12.004

Cheung, S.G., 1993. Population dynamics and energy budgets of green-lipped mussel *Perna viridis* (Linnaeus) in a polluted harbour. Journal of Experimental Marine Biology and Ecology 168, 1–24. https://doi.org/10.1016/0022-0981(93)90113-3

de Lafontaine, Y., Gagné, F., Blaise, C., Costan, G., Gagnon, P., Chan, H.M., 2000. Biomarkers in zebra mussels (*Dreissena polymorpha*) for the assessment and monitoring of water quality of the St Lawrence River (Canada). Aquatic toxicology 50, 51–71.

Directive 2000/60/EC du Parlement Européen et du Conseil du 23 octobre 2000 établissant un cadre pour une politique communautaire dans le domaine de l'eau (2000).

Eisner, V., Picard, M., Hajnóczky, G., 2018. Mitochondrial dynamics in adaptive and maladaptive cellular stress responses. Nat Cell Biol 20, 755–765. https://doi.org/10.1038/s41556-018-0133-0

Eprintsev, A.T., Fedorin, D.N., Dobychina, M.A., Igamberdiev, A.U., 2018. Regulation of expression of the mitochondrial and peroxisomal forms of citrate synthase in maize during germination and in response to light. Plant Science 272, 157–163. https://doi.org/10.1016/j.plantsci.2018.04.017

Falfushynska, H., Gnatyshyna, L., Yurchak, I., Ivanina, A., Stoliar, O., Sokolova, I., 2014. Habitat pollution and thermal regime modify molecular stress responses to elevated temperature in freshwater

mussels (*Anodonta anatina*: Unionidae). Science of The Total Environment 500–501, 339–350. https://doi.org/10.1016/j.scitotenv.2014.08.112

Fanslow, D.L., Nalepa, T.F., Johengen, T.H., 2001. Seasonal changes in the respiratory electron transport system (ETS) and respiration of the zebra mussel, *Dreissena polymorpha* in Saginaw Bay, Lake Huron. Hydrobiologia 448, 61–70.

Faria, M., Carrasco, L., Diez, S., Riva, M.C., Bayona, J.M., Barata, C., 2009. Multi-biomarker responses in the freshwater mussel *Dreissena polymorpha* exposed to polychlorobiphenyls and metals. Comparative Biochemistry and Physiology Part C: Toxicology & Pharmacology 149, 281–288. https://doi.org/10.1016/j.cbpc.2008.07.012

Faria, M., Navarro, A., Luckenbach, T., Piña, B., Barata, C., 2011. Characterization of the multixenobiotic resistance (MXR) mechanism in embryos and larvae of the zebra mussel (*Dreissena polymorpha*) and studies on its role in tolerance to single and mixture combinations of toxicants. Aquatic Toxicology 101, 78–87. https://doi.org/10.1016/j.aquatox.2010.09.004

Frederich, M., Balschi, J.A., 2002. The Relationship between AMP-activated Protein Kinase Activity and AMP Concentration in the Isolated Perfused Rat Heart. Journal of Biological Chemistry 277, 1928–1932. https://doi.org/10.1074/jbc.M107128200

Frieder, C.A., Applebaum, S.L., Pan, T.-C.F., Hedgecock, D., Manahan, D.T., 2017. Metabolic cost of calcification in bivalve larvae under experimental ocean acidification. ICES Journal of Marine Science 74, 941–954. https://doi.org/10.1093/icesjms/fsw213

Garaud, M., Auffan, M., Devin, S., Felten, V., Pagnout, C., Pain-Devin, S., Proux, O., Rodius, F., Sohm, B., Giamberini, L., 2016. Integrated assessment of ceria nanoparticle impacts on the freshwater bivalve *Dreissena polymorpha*. Nanotoxicology 10, 935–944. https://doi.org/10.3109/17435390.2016.1146363

Gist, D.H., Miller, M.C., Brence, W.A., 1997. Annual reproductive cycle of the zebra mussel in the Ohio River: a comparison with Lake Erie. Arch. Hydrobiol. 138, 365–379.

Han, H.-S., Kang, G., Kim, J.S., Choi, B.H., Koo, S.-H., 2016. Regulation of glucose metabolism from a liver-centric perspective. Exp Mol Med 48, e218–e218. https://doi.org/10.1038/emm.2015.122

Hassan, M.M., Qin, J.G., Li, X., 2018. Gametogenesis, sex ratio and energy metabolism in *Ostrea angasi*: implications for the reproductive strategy of spermcasting marine bivalves. Journal of Molluscan Studies 84, 38–45. https://doi.org/10.1093/mollus/eyx041

Hochaka and Somero, 2002. Biochemical adaptation: Mechanism and process in physiological evolution. Biochem. Mol. Biol. Educ. 30, 215–216. https://doi.org/10.1002/bmb.2002.494030030071

Hong, H.-K., Jeung, H.-D., Kang, H.-S., Choi, K.-S., 2020. Seasonal variations in the hemocyte parameters, gonad development, energy storage and utilization of the giant honeycomb oyster *Hyotissa hyotis* (Linnaeus 1758) in Jeju Island off the south coast of Korea. Aquaculture Reports 17, 100299. https://doi.org/10.1016/j.aqrep.2020.100299

Hraoui, G., Bettinazzi, S., Gendron, A.D., Boisclair, D., Breton, S., 2020. Mitochondrial thermo-sensitivity in invasive and native freshwater mussels. J Exp Biol 223, jeb215921. https://doi.org/10.1242/jeb.215921

Hrdinka, T., Novický, O., Hanslík, E., Rieder, M., 2012. Possible impacts of floods and droughts on water quality. Journal of Hydro-environment Research 6, 145–150. https://doi.org/10.1016/j.jher.2012.01.008

IPCC, 2014. In: Pachauri, R.K., Meyer, L.A. (Eds.), Climate Change 2014: Synthesis Report. Contribution of Working Groups I, II and III to the Fifth Assessment Report of the Intergovernmental Panel on Climate Change. IPCC, Geneva, Switzerland. Core Writing Team

Jost, J.A., Keshwani, S.S., Abou-Hanna, J.J., 2015. Activation of AMP-activated protein kinase in response to temperature elevation shows seasonal variation in the zebra mussel, *Dreissena polymorpha*. Comparative Biochemistry and Physiology Part A: Molecular & Integrative Physiology 182, 75–83. https://doi.org/10.1016/j.cbpa.2014.11.025

Juhel, G., Davenport, J., O'Halloran, J., Culloty, S.C., O'Riordan, R.M., James, K.F., Furey, A., Allis, O., 2006. Impacts of microcystins on the feeding behaviour and energy balance of zebra mussels, *Dreissena polymorpha*: A bioenergetics approach. Aquatic Toxicology 79, 391–400. https://doi.org/10.1016/j.aquatox.2006.07.007

Kerambrun, E., Delahaut, L., Geffard, A., David, E., 2018. Differentiation of sympatric zebra and quagga mussels in ecotoxicological studies: A comparison of morphometric data, gene expression, and body metal concentrations. Ecotoxicology and Environmental Safety 154, 321–328. https://doi.org/10.1016/j.ecoenv.2018.02.051

Kerambrun, E., Rioult, D., Delahaut, L., Evariste, L., Pain-Devin, S., Auffret, M., Geffard, A., David, E., 2016. Variations in gene expression levels in four European zebra mussel, *Dreissena polymorpha*, populations in relation to metal bioaccumulation: A field study. Ecotoxicology and Environmental Safety 134, 53–63. https://doi.org/10.1016/j.ecoenv.2016.08.018

Kurochkin, I.O., Etzkorn, M., Buchwalter, D., Leamy, L., Sokolova, I.M., 2011. Top-down control analysis of the cadmium effects on molluscan mitochondria and the mechanisms of cadmium-induced mitochondrial dysfunction. American Journal of Physiology-Regulatory, Integrative and Comparative Physiology 300, R21–R31. https://doi.org/10.1152/ajpregu.00279.2010

Kwan, K.H.M., Chan, H.M., De Lafontaine, Y., 2003. Metal contamination in zebra mussels (*Dreissena polymorpha*) along the St. Lawrence River. Environmental Monitoring and Assessment 88, 193–219. https://doi.org/10.1023/A:1025517007605

Lane N. 2005. Power, sex, suicide: mitochondria and the meaning of life. New York (NY): Oxford University Press. p. 368.

Lane, N., 2007. Mitochondria: Key to Complexity, in: Martin, W.F., Müller, M. (Eds.), Origin of Mitochondria and Hydrogenosomes. Springer Berlin Heidelberg, Berlin, Heidelberg, pp. 13–38. https://doi.org/10.1007/978-3-540-38502-8_2

Lannig, G., Cherkasov, A.S., Sokolova, I.M., 2006. Temperature-dependent effects of cadmium on mitochondrial and whole-organism bioenergetics of oysters (*Crassostrea virginica*). Marine Environmental Research 62, S79–S82. https://doi.org/10.1016/j.marenvres.2006.04.010

Le Gal, Y., Lagadic, L., Le Bras, S., Caquet, TH., 1998. Charge énergétique en adénylates (CEA) et autres biomarqueurs associés au métabolisme énergétique. In: Les biomarqueurs dans l'évaluation de l'état écologique des milieux aquatiques, Chap 12. Lavoisier.

Louis, F., Devin, S., Giambérini, L., Potet, M., David, E., Pain-Devin, S., 2019. Energy allocation in two dreissenid species under metal stress. Environmental Pollution 245, 889–897. https://doi.org/10.1016/j.envpol.2018.11.079

Lushchak, V.I., 2011. Environmentally induced oxidative stress in aquatic animals. Aquatic Toxicology 101, 13–30. https://doi.org/10.1016/j.aquatox.2010.10.006

Mackie, G.L., Ontario (Eds.), 1990. The Zebra mussel, *Dreissena polymorpha*: a synthesis of European experiences and a preview for North America. Ontario Environment, Ottawa.

Majumdar, D., Gupta, N., 2000. Nitrate pollution of groundwater and associated human health disorders. Indian Journal of Environmental Health 13.

McMahon, R.F., 2002. Evolutionary and physiological adaptations of aquatic invasive animals: *r* selection versus resistance. Canadian Journal of Fisheries and Aquatic Sciences 59, 1235–1244. https://doi.org/10.1139/f02-105

Monlun, M., Hyernard, C., Blanco, P., Lartigue, L., Faustin, B., 2017. Mitochondria as Molecular Platforms Integrating Multiple Innate Immune Signalings. Journal of Molecular Biology 429, 1–13. https://doi.org/10.1016/j.jmb.2016.10.028

Naquet, P., Giessner, C., Galland, F., 2016. Metabolic adaptation of tissues to stress releases metabolites influencing innate immunity. Current Opinion in Immunology 38, 30–38. https://doi.org/10.1016/j.coi.2015.10.005

Navarro, A., Faria, M., Barata, C., Piña, B., 2011. Transcriptional response of stress genes to metal exposure in zebra mussel larvae and adults. Environmental Pollution 159, 100–107. https://doi.org/10.1016/j.envpol.2010.09.018

O'Brien, W.G., Ling, H.S., Zhao, Z., Lee, C.C., 2017. New insights on the regulation of the adenine nucleotide pool of erythrocytes in mouse models. PLoS ONE 12, e0180948. https://doi.org/10.1371/journal.pone.0180948

Pain, S., Parant, M., 2007. Identification of multixenobiotic defence mechanism (MXR) background activities in the freshwater bivalve *Dreissena polymorpha* as reference values for its use as biomarker in contaminated ecosystems. Chemosphere 67, 1258–1263. https://doi.org/10.1016/j.chemosphere.2006.11.017

Palais, F., Mouneyrac, C., Dedourge-Geffard, O., Giambérini, L., Biagianti-Risbourg, S., Geffard, A., 2011. One-year monitoring of reproductive and energy reserve cycles in transplanted zebra mussels (*Dreissena polymorpha*). Chemosphere 83, 1062–1073. https://doi.org/10.1016/j.chemosphere.2011.01.060

Petes, L.E., Menge, B.A., Harris, A.L., 2008. Intertidal mussels exhibit energetic trade-offs between reproduction and stress resistance. Ecological Monographs 78, 387–402. https://doi.org/10.1890/07-0605.1

Pfaffl, M.W., 2001. A new mathematical model for relative quantification in real-time RT-PCR. Nucleic Acids Research 29, 45e–445. https://doi.org/10.1093/nar/29.9.e45

Plaistow, S.J., Troussard, J.-P., Cézilly, F., 2001. The effect of the acanthocephalan parasite *Pomphorhynchus laevi*s on the lipid and glycogen content of its intermediate host *Gammarus pulex*. International Journal for Parasitology 31, 346–351. https://doi.org/10.1016/S0020-7519(01)00115-1

Potet, M., Devin, S., Pain-Devin, S., Rousselle, P., Giambérini, L., 2016. Integrated multi-biomarker responses in two dreissenid species following metal and thermal cross-stress. Environmental Pollution 218, 39–49. https://doi.org/10.1016/j.envpol.2016.08.025

Potet, M., Giambérini, L., Pain-Devin, S., Louis, F., Bertrand, C., Devin, S., 2018. Differential tolerance to nickel between *Dreissena polymorpha* and *Dreissena rostriformis bugensis* populations. Sci. Rep. 8. https://doi.org/10.1038/s41598-018-19228-x.

Ram, J.L., Crawford, G.W., Walker, J.U., Mojares, J.J., Patel, N., Fong, P.P., Kyozuka, K., 1993. Spawning in the zebra mussel (*Dreissena polymorpha*): activation by internal or external application of serotonin. Journal of Experimental Zoology Part A: Ecological Genetics and Physiology 265, 587–598.

Ram, J.L., Fong, P.P., Garton, D.W., 1996. Physiological aspects of zebra mussel reproduction: maturation, spawning, and fertilization. American Zoologist 36, 326–338.

Ramcharan, C.W., Padilla, D.K., Dodson, S.I., 1992. Models to Predict Potential Occurrence and Density of the Zebra Mussel, *Dreissena polymorpha*. Can. J. Fish. Aquat. Sci. 49, 2611–2620. https://doi.org/10.1139/f92-289

Ricci, J.-E., Muñoz-Pinedo, C., Fitzgerald, P., Bailly-Maitre, B., Perkins, G.A., Yadava, N., Scheffler, I.E., Ellisman, M.H., Green, D.R., 2004. Disruption of Mitochondrial Function during Apoptosis Is Mediated by Caspase Cleavage of the p75 Subunit of Complex I of the Electron Transport Chain. Cell 117, 773–786. https://doi.org/10.1016/j.cell.2004.05.008

Salin, K., Auer, S.K., Rey, B., Selman, C., Metcalfe, N.B., 2015. Variation in the link between oxygen consumption and ATP production, and its relevance for animal performance. Proc. R. Soc. B 282, 20151028. https://doi.org/10.1098/rspb.2015.1028

Sharma, A.K., Singh, V., Gera, R., Purohit, M.P., Ghosh, D., 2017. Zinc Oxide Nanoparticle Induces Microglial Death by NADPH-Oxidase-Independent Reactive Oxygen Species as well as Energy Depletion. Mol Neurobiol 54, 6273–6286. https://doi.org/10.1007/s12035-016-0133-7

Składanowski, A.C., Stepnowski, P., Kleszczyński, K., Dmochowska, B., 2005. AMP deaminase in vitro inhibition by xenobiotics. Environmental Toxicology and Pharmacology 19, 291–296. https://doi.org/10.1016/j.etap.2004.08.005

Smolders, R., Bervoets, L., De Coen, W., Blust, R., 2004. Cellular energy allocation in zebra mussels exposed along a pollution gradient: linking cellular effects to higher levels of biological organization. Environmental Pollution 129, 99–112. https://doi.org/10.1016/j.envpol.2003.09.027

Sokolov, E.P., Markert, S., Hinzke, T., Hirschfeld, C., Becher, D., Ponsuksili, S., Sokolova, I.M., 2019. Effects of hypoxia-reoxygenation stress on mitochondrial proteome and bioenergetics of the hypoxia-tolerant marine bivalve *Crassostrea gigas*. Journal of Proteomics 194, 99–111. https://doi.org/10.1016/j.jprot.2018.12.009

Sokolova, I., Lannig, G., 2008. Interactive effects of metal pollution and temperature on metabolism in aquatic ectotherms: implications of global climate change. Climate Research 37, 181–201. https://doi.org/10.3354/cr00764

Sokolova, I., Pörtner, H., 2001. Physiological adaptations to high intertidal life involve improved water conservation abilities and metabolic rate depression in *Littorina saxatilis*. Mar. Ecol. Prog. Ser. 224, 171–186. https://doi.org/10.3354/meps224171

Sokolova, I.M., Bock, C., Pörtner, H.-O., 2000. Resistance to freshwater exposure in White Sea *Littorina spp*. I: Anaerobic metabolism and energetics. Journal of Comparative Physiology B 170, 91–103.

Sokolova, I.M., Frederich, M., Bagwe, R., Lannig, G., Sukhotin, A.A., 2012. Energy homeostasis as an integrative tool for assessing limits of environmental stress tolerance in aquatic invertebrates. Marine Environmental Research 79, 1–15. https://doi.org/10.1016/j.marenvres.2012.04.003

Sokolova, I.M., Sokolov, E.P., Ponnappa, K.M., 2005. Cadmium exposure affects mitochondrial bioenergetics and gene expression of key mitochondrial proteins in the eastern oyster *Crassostrea virginica* Gmelin (Bivalvia: Ostreidae). Aquatic Toxicology 73, 242–255. https://doi.org/10.1016/j.aquatox.2005.03.016

Somero, G.N., 2010. The physiology of climate change: how potentials for acclimatization and genetic adaptation will determine “winners” and “losers.” Journal of Experimental Biology 213, 912–920. https://doi.org/10.1242/jeb.037473

Soon, T.K., Zheng, H., 2019. Climate Change and Bivalve Mass Mortality in Temperate Regions, in: de Voogt, P. (Ed.), Reviews of Environmental Contamination and Toxicology Volume 251. Springer International Publishing, Cham, pp. 109–129. https://doi.org/10.1007/398_2019_31

Spidle, A.P., May, B., Mills, E.L., 1995. Limits to tolerance of temperature and salinity in the quagga mussel (*Dreissena bugensis*) and the zebra mussel (*Dreissena polymorpha*). Can. J. Fish. Aquat. Sci. 52, 2108–2119. https://doi.org/10.1139/f95-804

Sprung, M., 1995. Physiological energetics of the zebra mussel *Dreissena polymorpha* in lakes III. Metabolism and net growth efficiency. Hydrobiologia 304, 147–158.

Tourari, A.L., Crochard, C., Pihan, J.C., 1988. Action de la température sur le cycle de reproduction de *Dreissena polymorpha* (Pallas). Etude ‘‘*in situ*’’ et au laboratoire. Haliotis 18, 85–98.

Vakifahmetoglu-Norberg, H., Ouchida, A.T., Norberg, E., 2017. The role of mitochondria in metabolism and cell death. Biochemical and Biophysical Research Communications 482, 426–431. https://doi.org/10.1016/j.bbrc.2016.11.088

van Handel, E., 1985. Rapid determination of total lipids in mosquitoes. J. Am. Mosq. Control Assoc. Vol 1 No. 3, 302-304

van Vliet, M.T.H., Zwolsman, J.J.G., 2008. Impact of summer droughts on the water quality of the Meuse river. Journal of Hydrology 353, 1–17. https://doi.org/10.1016/j.jhydrol.2008.01.001

Verslycke, T., Roast, S.D., Widdows, J., Jones, M.B., Janssen, C.R., 2004. Cellular energy allocation and scope for growth in the estuarine mysid *Neomysis integer* (Crustacea: Mysidacea) following chlorpyrifos exposure: a method comparison. Journal of Experimental Marine Biology and Ecology 306, 1–16. https://doi.org/10.1016/j.jembe.2003.12.022

Figure 1. Temperature continuously measured on sampling site. The mean, minimum and maximum temperature are presented.

Figure 2. Gonadal development stage for males (A) and females (B) according to the months. Different development stages are presented in terms of percentage of each stage (*n*=12).

Figure 3. Condition index (*n*=60) (A), glycogen (B), lipids (C) and proteins (D) content (*n*=12) according to the months. Data are presented as median ± SD, min, max. Different letters indicate significant differences between months ($p < 0.05$).

Figure 4. CS (A), COX (B) and ETS (C) activities according to the months. Data are presented as median ± SD, min, max (*n*=12). Different letters indicate significant differences between months ($p < 0.05$).

Figure 5. *atp* (A), *cox* (B), *cytb* (C) and *cs* (D) relative gene expression levels according to the months. Data are presented as median ± SD, min, max (*n*=12). Different letters indicate significant differences between months ($p < 0.05$).

Figure 6. *ampk* (A) and *ampd* (B) relative gene expression levels according to the months. Data are presented as median ± SD, min, max (*n*=12). Different letters indicate significant differences between months ($p < 0.05$).

Figure 7. Part I: ATP (A), ADP (B), AMP (C) and IMP (D) contents. Part II: adenylate energy charge (AEC). Results are presented according to the months and data are expressed as median ± SD, min, max (*n*=12). Different letters indicate significant differences between months ($p < 0.05$).

Figure 8. *ldh* relative gene expression level (A), LDH activity (B), *aox* relative gene expression level (C), lipid peroxidation (LOOH) (D) and caspase-3 activity (E) according to

the months. Data are expressed as median ± SD, min, max (*n*=12). Different letters indicate significant differences between months ($p < 0.05$).

Figure 9. Hierarchical cluster analysis (complete linkage using Euclidean distance measures) applied on the PLS model. The values in the similarity matrix can be seen as a robust approximation of the Pearson correlation. The rows and columns were reordered according to some hierarchical clustering method to identify interesting patterns. SM: suspended matter; COD: chemical oxygen demand.

Supplementary data:

Figure S1. *sdh* gene expression level according to the months. Data are expressed as median ± SD, min, max (*n*=12). Different letters indicate significant differences between months ($p < 0.05$).

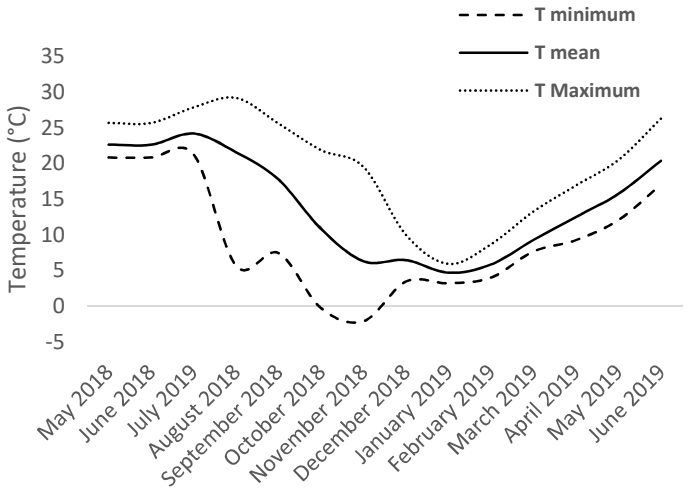
T minimum
T mean
T Maximum
Temperature (°C)
35
30
25
20
15
10
5
0
-5
May 2018
June 2018
July 2019
August 2018
September 2018
October 2018
November 2018
December 2018
January 2019
February 2019
March 2019
April 2019
May 2019
June 2019

Figure 1.

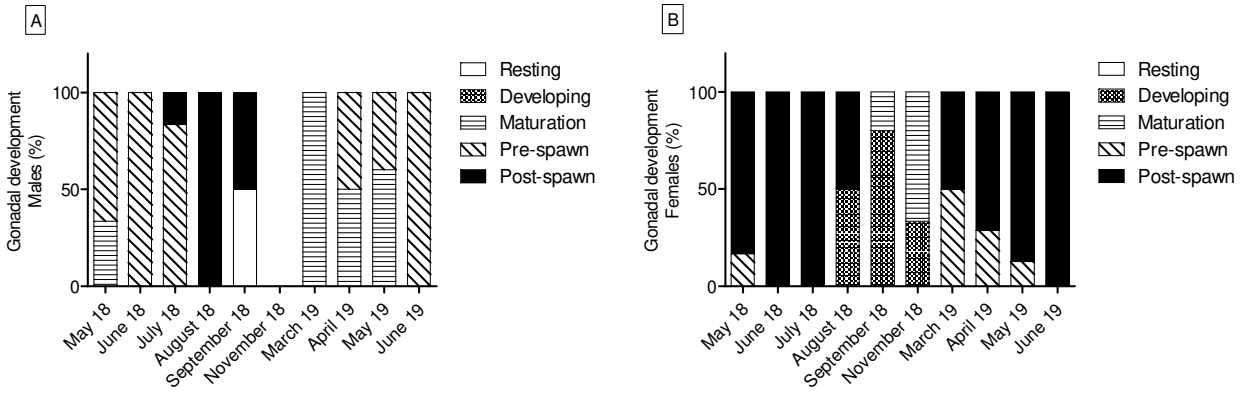
A
Gonadal development
Males (%)
100
50
0
May 18
June 18
July 18
August 18
September 18
November 18
March 19
April 19
May 19
June 19
Resting
Developing
Maturation
Pre-spawn
Post-spawn
B
Gonadal development
Females (%)
100
50
0
May 18
June 18
July 18
August 18
September 18
November 18
March 19
April 19
May 19
June 19
Resting
Developing
Maturation
Pre-spawn
Post-spawn

Figure 2.

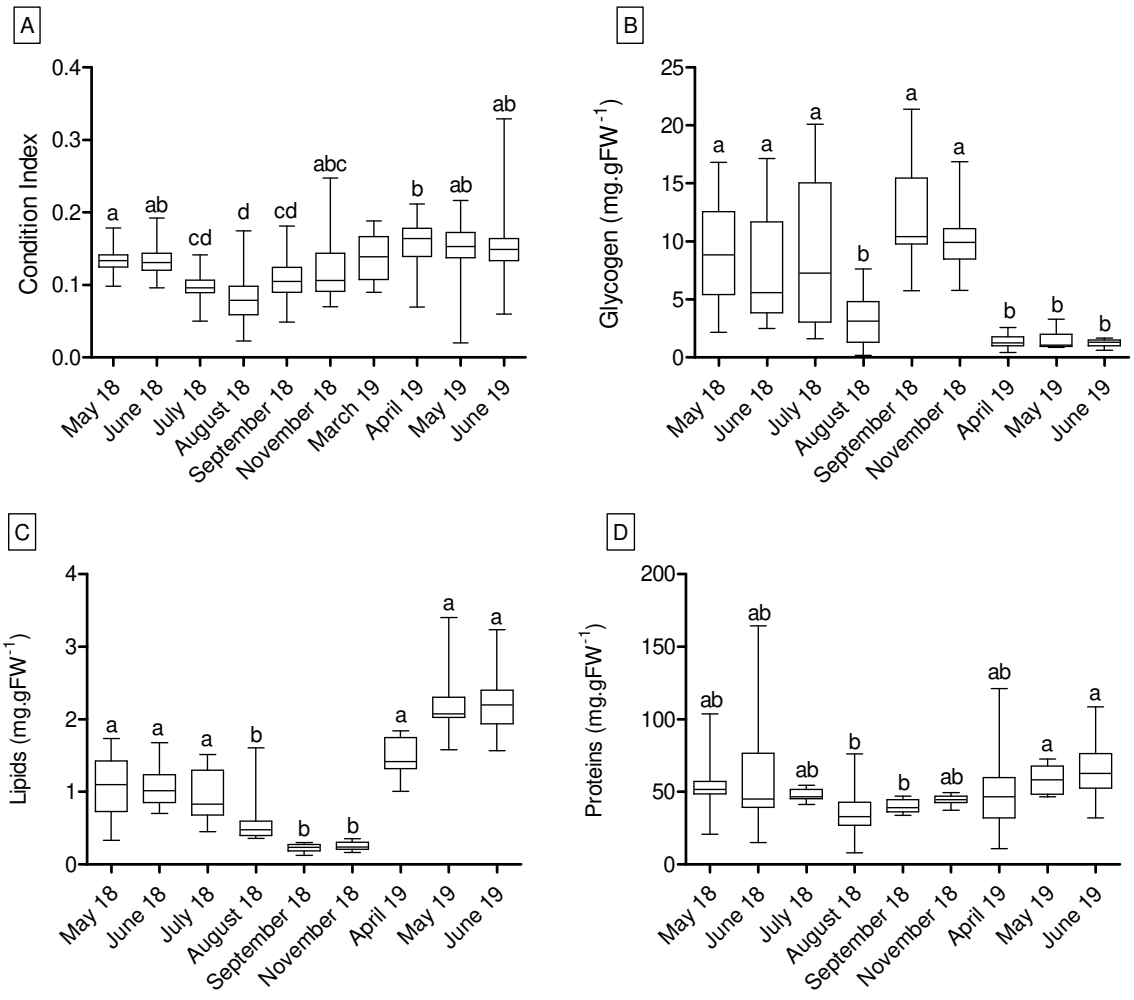
A
Condition Index
0.4
0.3
0.2
0.1
0.0
a
ab
cd
d
cd
abc
b
ab
ab
May 18
June 18
July 18
August 18
September 18
November 18
March 19
April 19
May 19
June 19
B
Glycogen (mg.gFW-1)
25
20
15
10
5
0
a
a
a
b
a
a
b
b
b
May 18
June 18
July 18
August 18
September 18
November 18
April 19
May 19
June 19
C
Lipids (mg.gFW-1)
4
3
2
1
0
a
a
a
b
b
b
a
a
a
May 18
June 18
July 18
August 18
September 18
November 18
April 19
May 19
June 19
D
Proteins (mg.gFW-1)
200
150
100
50
0
ab
ab
ab
b
b
ab
ab
a
a
May 18
June 18
July 18
August 18
September 18
November 18
April 19
May 19
June 19

Figure 3.

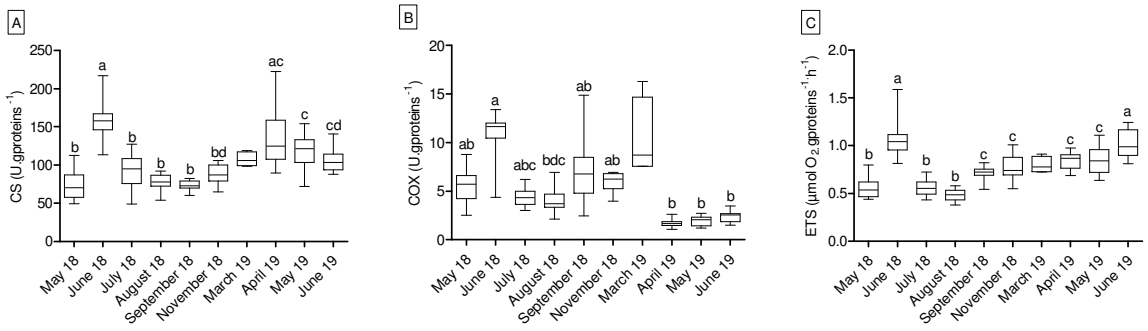
A
CS (U.gproteins-1)
250
200
150
100
50
0
b
a
b
b
b
bd
ac
c
cd
May 18
June 18
July 18
August 18
September 18
November 18
March 19
April 19
May 19
June 19
B
COX (U.gproteins-1)
20
15
10
5
0
ab
a
abc
bdc
ab
ab
b
b
b
C
ETS (µmol O2.gproteins-1.h-1)
2.0
1.5
1.0
0.5
0.0
b
a
b
b
c
c
c
c
a

Figure 4.

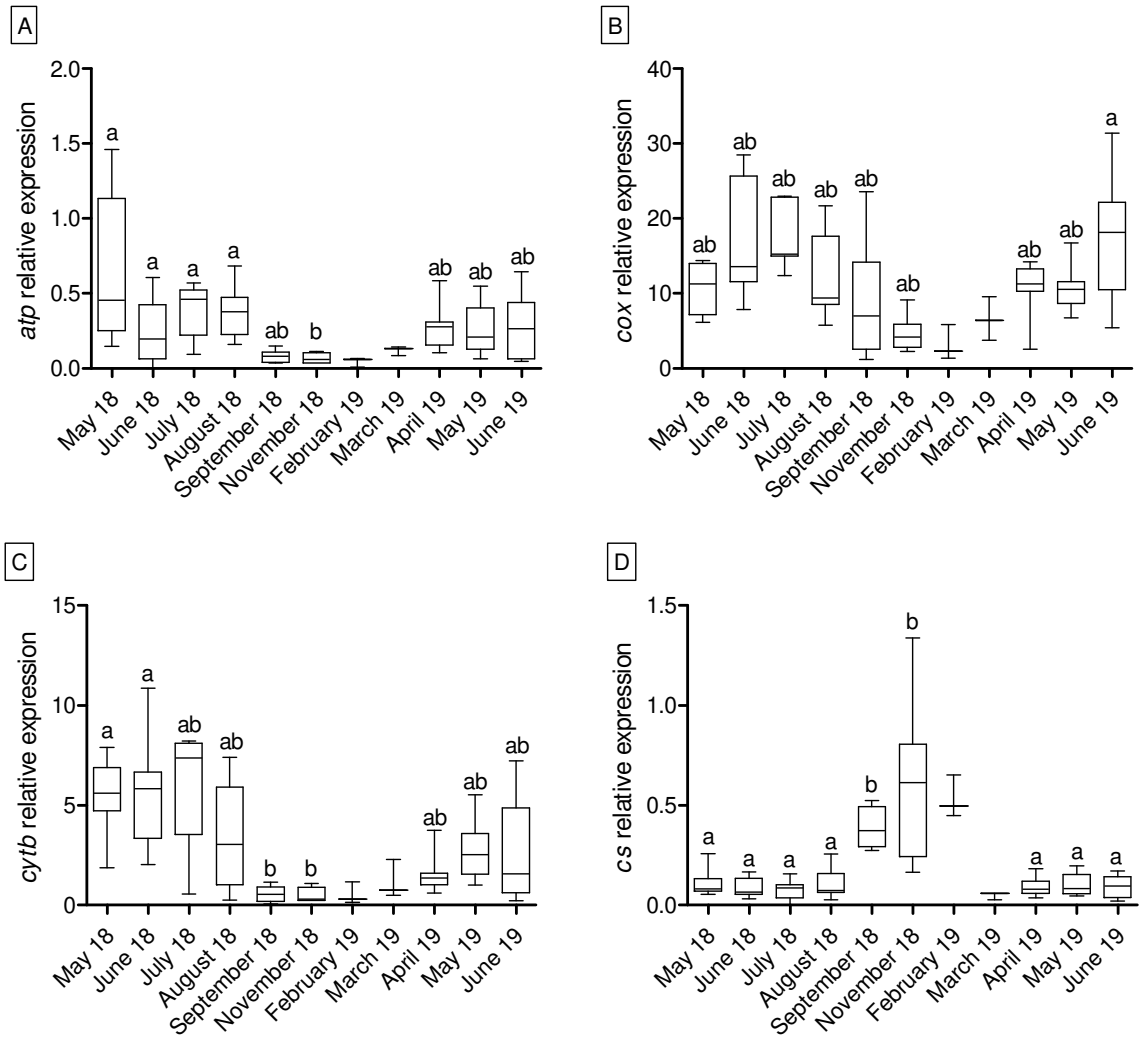
A
atp relative expression
2.0
1.5
1.0
0.5
0.0
a
a
a
a
ab
b
ab
ab
ab
May 18
June 18
July 18
August 18
September 18
November 18
February 19
March 19
April 19
May 19
June 19
B
cox relative expression
40
30
20
10
0
ab
ab
ab
ab
ab
ab
a
ab
ab
C
cytb relative expression
15
10
5
0
a
a
ab
ab
b
b
ab
ab
ab
D
cs relative expression
1.5
1.0
0.5
0.0
a
a
a
a
b
b
a
a
a

Figure 5.

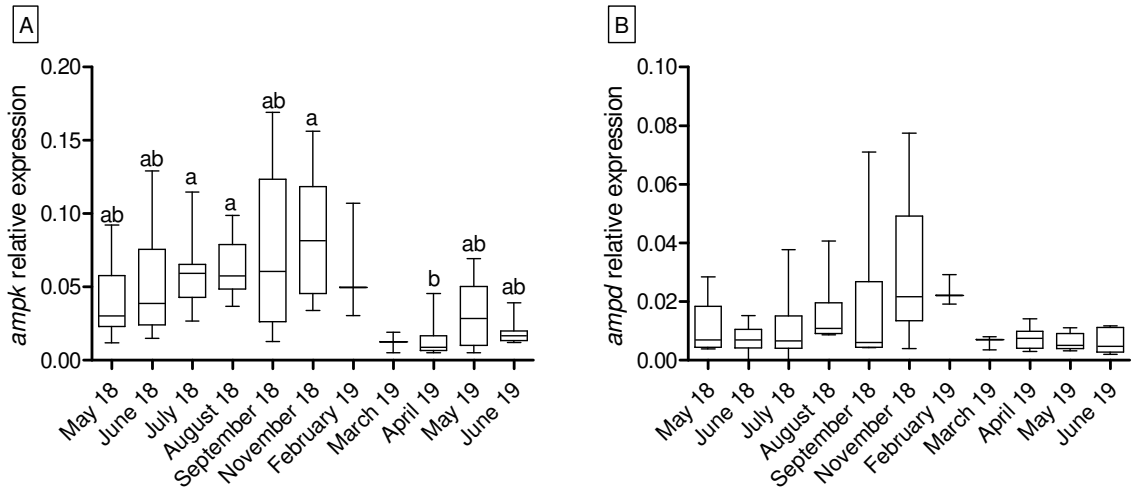
A
ampk relative expression
0.20
0.15
0.10
0.05
0.00
ab
ab
a
a
ab
a
b
ab
ab
May 18
June 18
July 18
August 18
September 18
November 18
February 19
March 19
April 19
May 19
June 19
B
ampd relative expression
0.10
0.08
0.06
0.04
0.02
0.00
May 18
June 18
July 18
August 18
September 18
November 18
February 19
March 19
April 19
May 19
June 19

Figure 6.

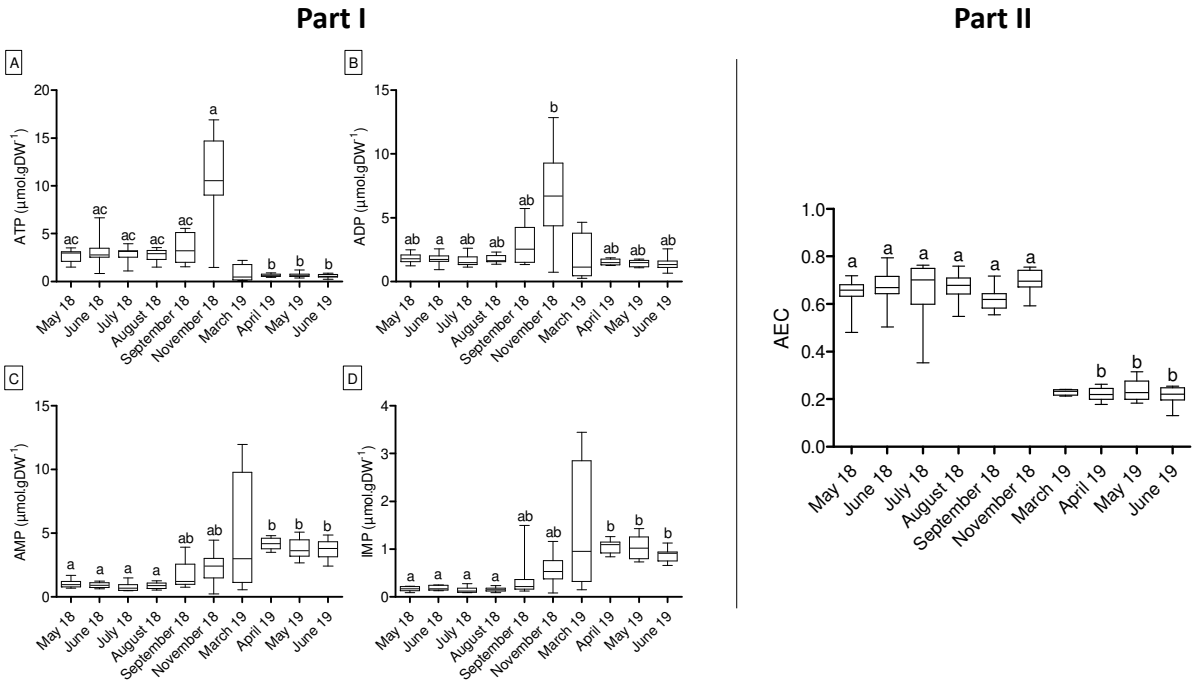
Part I
Part II
A
B
C
D
ATP (µmol.gDW-1)
ADP (µmol.gDW-1)
AMP (µmol.gDW-1)
IMP (µmol.gDW-1)
AEC
May 18
June 18
July 18
August 18
September 18
November 18
March 19
April 19
May 19
June 19

Figure 7.

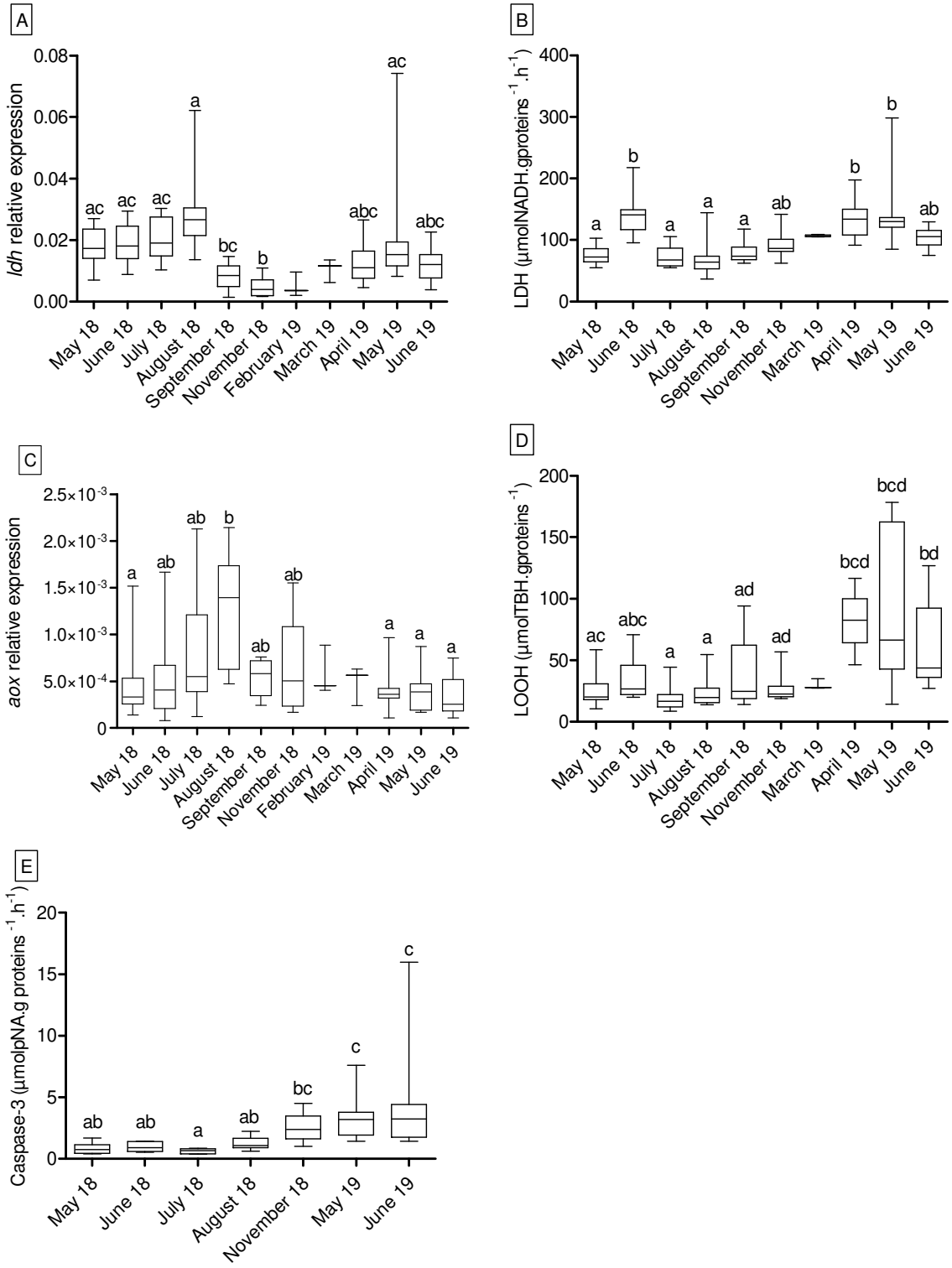
A
idh relative expression
0.08
0.06
0.04
0.02
0.00
ac ac ac a bc b abc ac abc
May 18 June 18 July 18 August 18 September 18 November 18 February 19 March 19 April 19 May 19 June 19
B
LDH (µmolNADH.gproteins-1.h-1)
400
300
200
100
0
a b a a a ab b ab
May 18 June 18 July 18 August 18 September 18 November 18 March 19 April 19 May 19 June 19
C
aox relative expression
2.5×10-3
2.0×10-3
1.5×10-3
1.0×10-3
5.0×10-4
0
a ab ab b ab ab a a a
May 18 June 18 July 18 August 18 September 18 November 18 February 19 March 19 April 19 May 19 June 19
D
LOOH (µmolTBH.gproteins-1)
200
150
100
50
0
ac abc a a ad ad bcd bcd bd
May 18 June 18 July 18 August 18 September 18 November 18 March 19 April 19 May 19 June 19
E
Caspase-3 (µmolpNA.g proteins-1.h-1)
20
15
10
5
0
ab ab a ab bc c c
May 18 June 18 July 18 August 18 November 18 May 19 June 19

Figure 8.

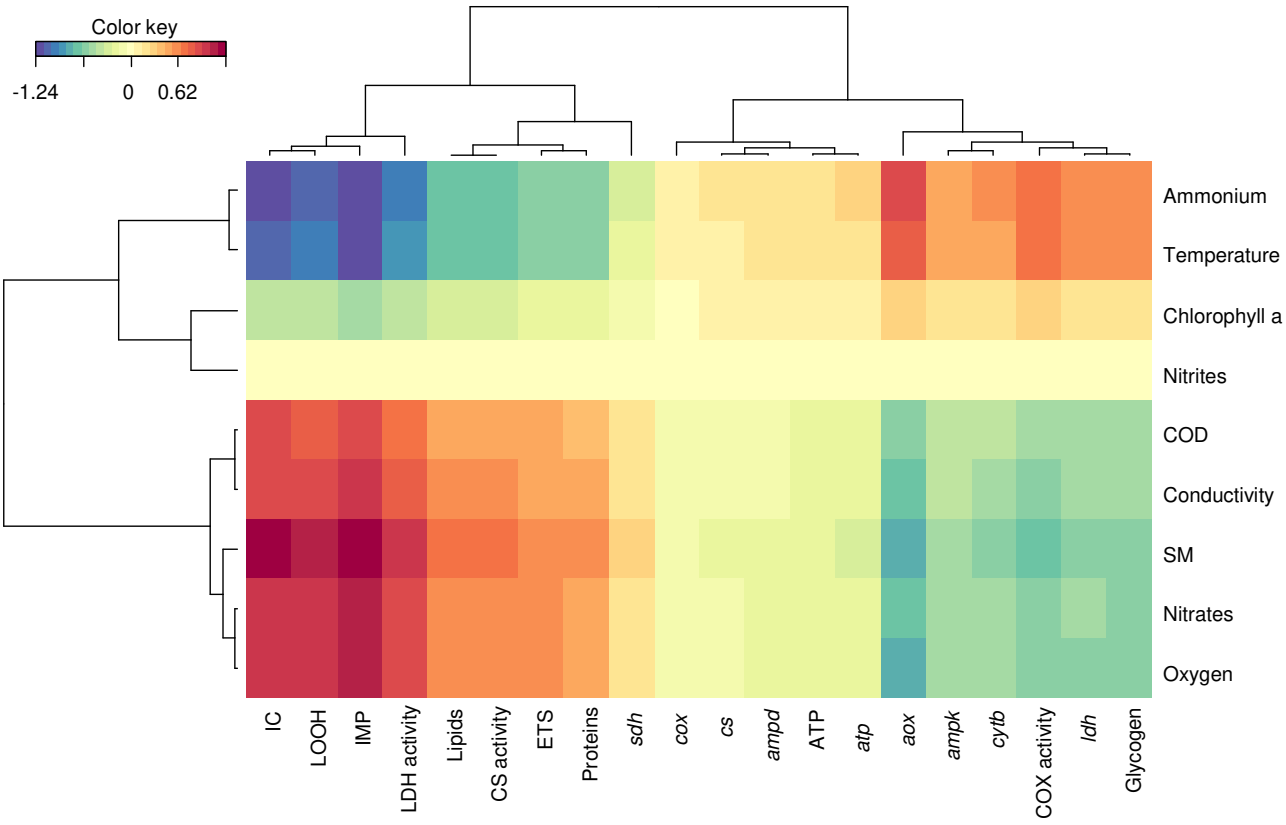
Color key
-1.24
0
0.62
Ammonium
Temperature
Chlorophyll a
Nitrites
COD
Conductivity
SM
Nitrates
Oxygen
IC
LOOH
IMP
LDH activity
Lipids
CS activity
ETS
Proteins
sdh
cox
cs
ampd
ATP
atp
aox
ampk
cytb
COX activity
ldh
Glycogen

Figure 9.

Supplementary data :

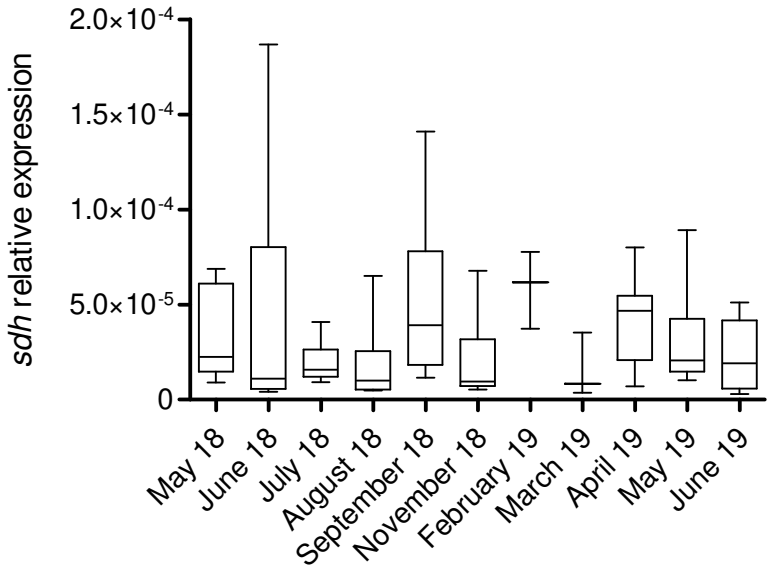

Figure S1.

Table 1. Summary of the primers used for gene expression measurements. Abbreviations, NCBI accession numbers of the original sequences of the target genes in *D. polymorpha.*

Gene	Abbreviation	NCBI	F primers	R primers
Actin	*act*	AF082863	CCTCACCCTCAAGTACCCCAT	TTGGCCTTTGGGTTGAGTG
Alternative oxidase	*aox*	Q9P959	GTGAACCATACCCTCGCCTC	TGTAGTGACTGCGGATGGTC
AMP deaminase	*ampd*	Q9DBT5	ACCCAGCCAGTGTTGTTTCA	TTTGCTCGTGGACTCAACGT
AMP kinase α subunit	*ampk*	Q8BRK8	TGCTAAATGAAAGAGGTGACGC	CATGTGGTGGCATATACGATGT
ATP synthase	*atp*	JQ781135	GACTCCACCTCCCGTATCCT	TCCTCTGAAAGCTCGTCCAT
Citrate synthase	*cs*	MN579511	GTGCCCTGTCAGACCCTTAC	CTGTCCTGCCTTGAGTGTGT
Cytochrome b	*cytb*	DQ072120.1	CGCCACTTTAAAGCGATTTTT	TGGGTCAGCAAATAGATCTGG
Cytochrome c oxidase	*cox*	AAL55513	AGGCCCTGCGATAGATTTTT	AAAGGGACCCGGTAAAATTG
Lactate dehydrogenase	*ldh*	Q7TNG8	TGCCCAAACTACATTGCCAAAT	ATTGGGATTGGCAAACGGGA
Ribosomal protein S3	*s3*	AJ517687	CAGTGTGAGTCCCTGAGATACAAG	AACTTCATGGACTTGGCTCTCTG
Succinate dehydrogenase	*sdh*	Q9YHT2	TAGACCGTCCAGTTTAGCGC	CCTCTGCCACACATGTACGT

Table 2. Environmental parameters recorded *in situ* or in water samples: water physico-chemistry and contamination measurements; dO_2: dissolved oxygen; SM: suspended matter; COD: chemical oxygen demand; NO_2^-: nitrites; NO_3^-: nitrates; NH_4^+: ammonium; Chl a: chlorophyll a; ND: not detected.

Month	Temperature (°C)	Conductivity ($\mu S.cm^{-1}$)	dO_2 ($mg.L^{-1}$)	SM ($mg.L^{-1}$)	COD ($mg.L^{-1}$)	NO_2^- ($mg.L^{-1}$)	NO_3^- ($mg.L^{-1}$)	NH_4^+ ($mg.L^{-1}$)	Chl a ($\mu g.L^{-1}$)	Hydrocarbon ($mg.L^{-1}$)
May-18	22.7	497	9.1	ND	15.5	0.14	18	0.14	0.2	ND
June-18	22.9	485	9.8	ND	17.4	0.08	15	0.10	0.4	ND
July-18	24.2	505	9.4	4	18.9	0.13	12	0.10	0.6	0.002
August-18	21.6	410	7.1	5	14.2	0.11	8	0.09	6.7	ND
September-18	17.8	410	9	8	14.2	0.13	7	0.07	2.7	ND
November-18	6.3	740	13	5	8.88	0.08	11	0.01	4.1	0.001
February-19	5.8	521	13.2	20	16.2	0.09	26	0.09	9.8	ND
March-19	9.3	491	10.7	24	16.5	0.12	19	0.19	1.9	ND
April-19	12.5	520	10.4	20	40.5	0.09	21	0.02	1.5	ND
May-19	15.8	547	9.7	25	11.7	0.19	14	0.04	ND	ND
June-19	20.4	527	9.6	20	13.8	0.1	13	0.09	ND	ND

Table 3. Pearson's correlations between the lipid peroxidation and the caspase-3 activity with the target markers for the total dataset. Only significant correlations for LOOH content and/or caspase activity are presented.

	Lipid peroxidation	Caspase-3 activity
	r^2	
Lipids	0.59	n.s
Glycogen	0.4	n.s
[AMP]	0.71	0.91
[IMP]	0.68	0.88
Condition Index (CI)	0.57	n.s
LDH activity	0.55	n.s
cytb gene expression	n.s	0.51

Supplementary data:

Table S1. Correlations of temperature and ATP content according to target markers of the total data set using multiple linear regression. Only significant correlations were presented.

	Temperature		[ATP]	
	p value	r^2	*p* value	r^2
cox gene expression	0.0159	0.43		
atp gene expression	0.0148	0.44		
cytb gene expression	0.001	0.66		
ldh gene expression	0.004	0.56		
cs gene expression	0.036	0.34	0.013	0.50
ampd gene expression			0.015	0.48
Lipids			0.019	0.50
Glycogen			0.025	0.47

Table S2. VIP values of PLS DA model built on biology responses. Only values ≥ 0.9 were presented.

Variable	VIP value
atp	1.23
ldh	1.19
cs	1.17
IC	1.12
cytb	1.05
ATP	1.03
LDH	1.02
IMP	1.02
ETS	1.02
LOOH	1.02
Lipids	0.99
ampd	0.99
aox	0.97
Proteins	0.92
ampk	0.91
cox	0.90

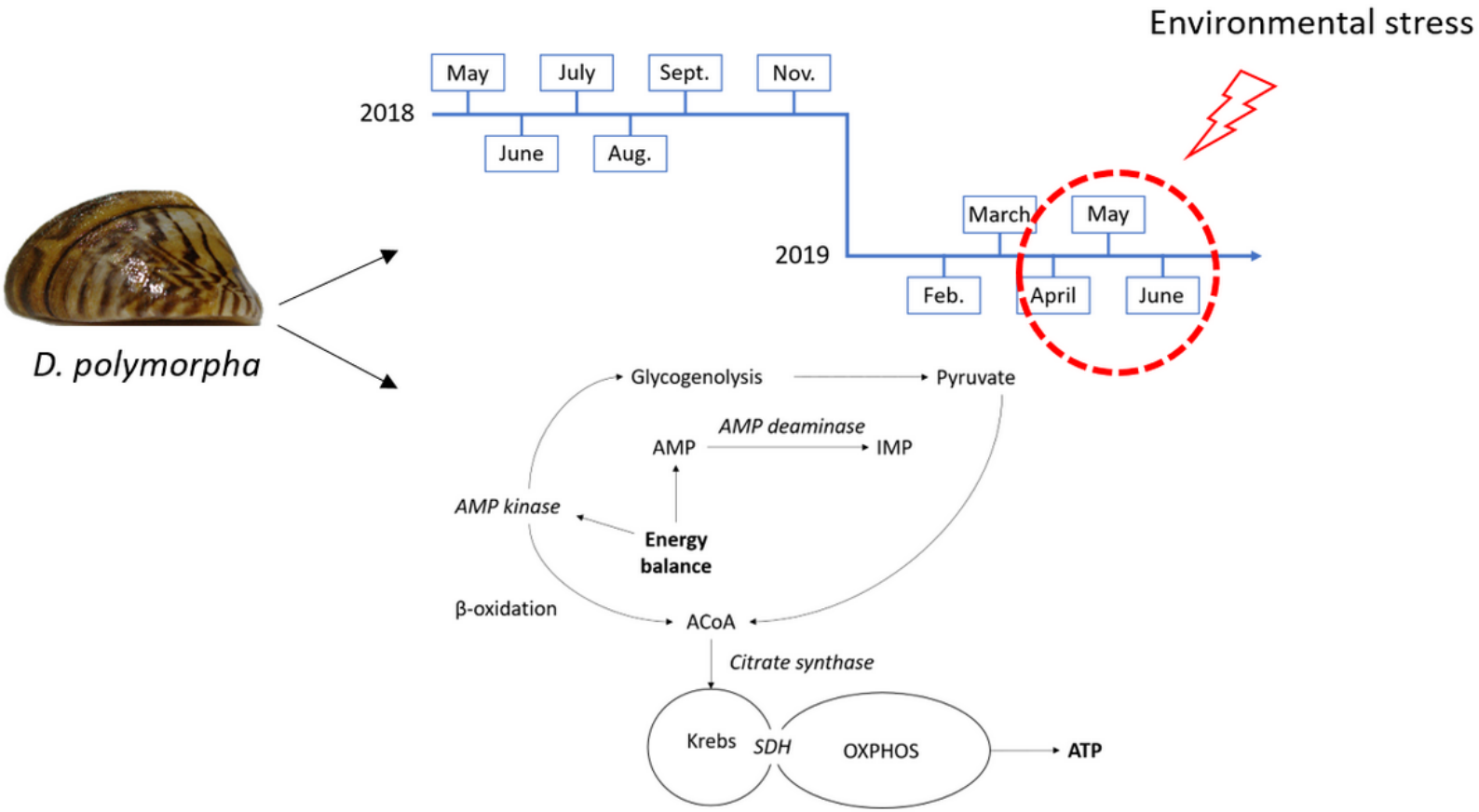
Environmental stress
2018
May
July
Sept.
Nov.
June
Aug.
2019
March
May
Feb.
April
June
D. polymorpha
Glycogenolysis
Pyruvate
AMP deaminase
AMP
IMP
AMP kinase
Energy balance
β-oxidation
ACoA
Citrate synthase
Krebs
SDH
OXPHOS
ATP